

# Biomechanics and Biotensegrity: Study Method and Frequency Response of the Simplex and 3-bar-SVD Tensegrity Configurations

C Castro Arenas<sup>1,2,4</sup>, I Gherzi<sup>2,3</sup>, M T Miralles<sup>2,3,4</sup>

<sup>1</sup> Centro Laboratorio de Morfología, Instituto de la Espacialidad Humana, Facultad de Arquitectura Diseño y Urbanismo, Universidad de Buenos Aires, Intendente Guiraldes 2160, Pabellón III, Ciudad Universitaria, CABA, Buenos Aires, Argentina.

<sup>2</sup> Centro de Investigación en Diseño Industrial de Productos Complejos, Facultad de Arquitectura Diseño y Urbanismo, Universidad de Buenos Aires, Intendente Guiraldes 2160, Pabellón III, Ciudad Universitaria, CABA, Buenos Aires, Argentina.

<sup>3</sup> Pontificia Universidad Católica Argentina (LaBIS-Facultad de Ciencias Fisicomatemáticas e Ingeniería-UCA), Av. A. Moreau de Justo 1500, CABA, Buenos Aires, Argentina.

e-mail: ccastroarenas@gmail.com, mmiralles@gmail.com

**Abstract.** The purpose of this work is to study the frequency response of 3D tensegrity structures. These are structures that have been used, since the 80's, to model biological systems of different scales. This fact led to the origin of the field of biotensegrity, which includes biomechanics as a natural field of application. In this work: a) A simple method for the analysis of frequency response of different nodes in 3D tensegrity structures was set up and tuned. This method is based on a video-analysis algorithm, which was applied to the structures, as they were vibrated along their axis of symmetry, at frequencies from 1 Hz to 60 Hz. b) Frequency-response analyses were performed, for the simplest 3D structure, the Simplex module, as well as for two towers, formed by stacking two and three Simplex modules, respectively. Resonant frequencies were detected for the Simplex module at  $(19.2 \pm 0.1)$  Hz and  $(50.2 \pm 0.1)$  Hz (the latter being an average of frequencies between homologous nodes). For the towers with two and three modules, each selected node presented a characteristic frequency response, modulated by their spatial placement in each model. Resonances for the two-stage tower were found at:  $(12 \pm 0.1)$  Hz;  $(16.2 \pm 0.1)$  Hz;  $(29.4 \pm 0.1)$  Hz and  $(37.2 \pm 0.1)$  Hz. For the tower with three Simplex modules, the main resonant frequencies were found at  $(12.0 \pm 0.1)$  Hz and  $(21.0 \pm 0.1)$  Hz. Results show that the proposed method is adequate for the study (2D) of any 3D tensegrity structure, with the potential of being generalized to the study of oscillations in three dimensions. A growing complexity and variability in the frequency response of the nodes was observed, as modules were added to the structures. These findings were compared to those found in the available literature.

## 1. Introduction

This paper aims to explore the applications that biotensegrity may have in areas of human biomechanics [1], both for modeling the behavior of well-known anatomical structures, as well as for

<sup>4</sup> Corresponding author



initiating preliminary studies on the still little explored dynamic behavior of these structures. The term “biotensegrity” was created by S. M. Levin, refers to the application of tensegrity principles to biological forms, with a focus on their structural and mechanical performance [2, 3]. This paper uses the term biotensegrity in a narrow sense, on one hand to denote the analogy between the biological structures bio-mechanical behavior, and on the other hand, the dynamic behavior of tensegrity structures.

Tensegrity defines class-specific structural systems in stable equilibrium known since the 50's [4]. These systems constitute spatial networks formed by independent interconnected tensors of traction and compression bars.

The interest in this type of study lies on the importance of geometry in relation to the mechanical properties of materials and, as well as on the need to have the quantity and quality of mass in specific parts of the structures, to support and pass the preset loads.

Specifically, tensegrity structures are material arrangements with low mass that adds the ability to replace other self-similar element of tensegrity, to achieve greater efficiency in their behavior. Dynamic knowledge, in particular frequency response, allows improving current theoretical models of control to implement the tensors with different types of sensors and replace the bars with actuators or active mechanical elements (smart tensegrity structures). D.E. Ingber argued that tensegrity is the fundamental architecture of life, based on his observations in cells [5]. Tensegrity structures possess relevant performance qualities such as flexibility, compactness, material optimization and resilience, extending its applications to different scales, manufacturing processes and materials. However, little is known about its dynamic properties.

There are numerous works on classification and mechanical behavior of the tensegrity simplest module, known either as “module Simplex” [4]. All members of a tensegrity structure are axially loaded. The overall structure is flexed with external static loads while no elements of the tensegrity structure flex in themselves.

The choice of the geometric parameters determines the mechanical properties having a great influence on the resistance of the structure. One of the most outstanding properties of these structures, of interest to biomechanics, is the increase in stiffness by load increase (unless a tensor is loosen) and to the fact that the shape of the structure can be changed with a minimum application of energy.

This paper presents the development of a simple method for studying response in frequency and resonance forms of different nodes of tensegrity vibration structures (up to 60 Hz), for a: a) Simplex module, b) 3-bar two stages SVD tensegrity, and, c) 3-bar three stages SVD tensegrity. The aim is to relate the findings with future models of biomechanics of lumbar spine for which two adjacent vertebrae and their interposed inter-vertebrae disk form a motion segment of the spine [6].

## 2. Methodology

### 2.1. Preparation of models

The Simplex tensegrity module is the minimal and simplest 3D tensegrity structure. It is composed by three bars and nine strings and is the basic module of 3-bar SVD tensegrity configurations. The 3-bar-SVD tensegrity (class 1), is comprised of three bars held together in space by strings. The strings supporting the next stage are known as the “saddle strings” (S). The strings connecting the top of the bars of one stage to the top of bars of the adjacent stages, or the bottom of the bars of one stage to the bottom of bars of the adjacent stages, are known as the “diagonal strings” (D). Strings connecting the top of the bars of one stage to the bottom of the bars of the same stage are known as “vertical strings” (V). It is a pre-tensed, self-supporting structure holding the position or stability in its vertices by the pre-stress (pre-existing stress tensor or isometric tension) of its own structure. From the biomechanics point of view, bones are analogous to bars that resist muscle traction, and those of tendon and ligament traction are related to tensors. Muscle tone (pre-stress) modulates the stability and stiffness of the body structure.

For this work, three models corresponding to a Simplex module (Figure 1a), a 3-bar two stages SVD tensegrity (Figure 1b) and a 3-bar three stages SVD tensegrity (Figure 1c) were built. The compression bars of the scale models were built in pieces of hollow aluminum bars (0.8 mm wall thickness) of  $(0.5 \pm 0.1)$  cm external diameter and  $(20 \pm 0.1)$  cm length. Commercial traction springs in three different lengths (at rest) and 4 different lengths (under tension) were used as links. The interconnection between springs and bars were made from metal anchors located at the ends of the bars.

## 2.2. Frequency Response and modes of vibration of the nodes in tensegrity structures

The models were placed on an acrylic square platform perforated with small in line holes, to lose weight and to allow the correct fixation of the structures to the uni-axial mechanical oscillator (Pasco Mech. Wave Driver SF-9324). The nodes of the studied structures were numbered consecutively and instrumented with Light Emitting Diodes (LEDs) in order to be properly identified, as shown in figure 1. The input signals were produced by a sine wave generator.

Given that the mechanical actuator has its own transfer function, for all cases a reference node for the models was defined (node), allowing to record the properties of base displacement. The marker movements were analyzed with respect to the position of this base marker, to its own spatial position in the structure and to the extent of effective displacement in the image plane (x-y plane).

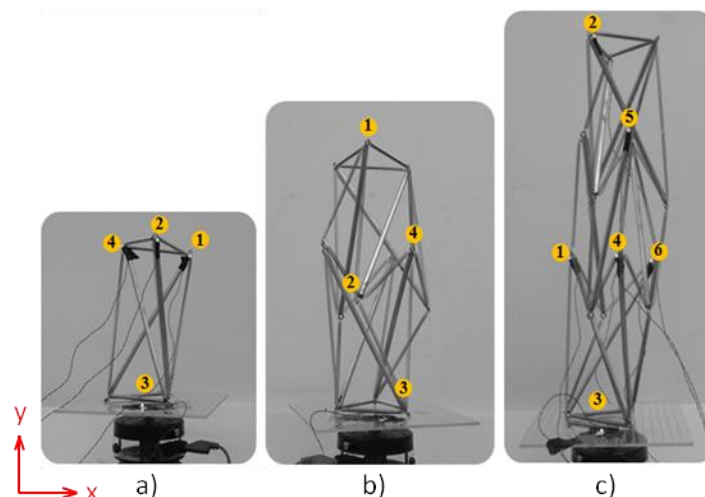


**Figure 1.** Models implemented with LEDs in nodes of interest. Shown: a) Simplex module; b) 3-bar two stages SVD tensegrity; and, c) 3-bar three stages SVD tensegrity. Numbers were independently assigned in each of the structures to denote nodes of interest in each case.

A sine wave signal generator (Pasco WA-9867) was used to power the mechanical oscillator. Its output was variable in frequency (0.1 Hz - 1000.0 Hz), and of controllable amplitude (0 V – 10 V). During the tests, inputs to the oscillator were kept constant in amplitude (50 %, 75 %), while their frequency was swept with the signal generator at  $(1.0 \pm 0.1)$  Hz steps. With a sampling rate of 120 fps for the camera, a frequency ramp was implemented, from 1.0 Hz to 60.0 Hz. The position of the markers at each frequency level was recorded by a high speed Casio EXFH25 camera, for 3 seconds.

The coordinates -in pixels- of the estimated centroid of each LED marker were acquired as a two-dimensional vector (x-axis: horizontal; y axis: vertical) for each table. The estimated path travelled by each marker was obtained from the timed succession of these coordinates. Figures 2 and 3 illustrate the above mentioned analysis for a three stages module that served to adjust the method. The sampling

frequency is high enough for maintaining an acceptable work resolution (640 x 480 pixels). The videos are stored in the memory of the camera, later retrieved and processed by a specific application for these studies.

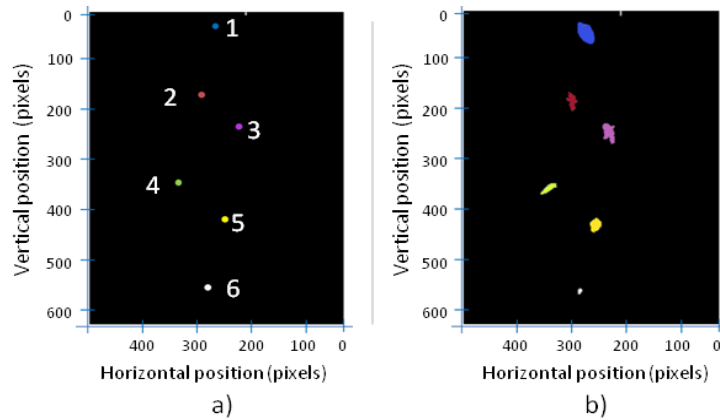


**Figure 2.** a) Test 3-bar three stages SVD tensegrity instrumented with LEDs in each of the six nodes, b) Image of the LEDs vibrating at its resonance frequency in the x-y plane.

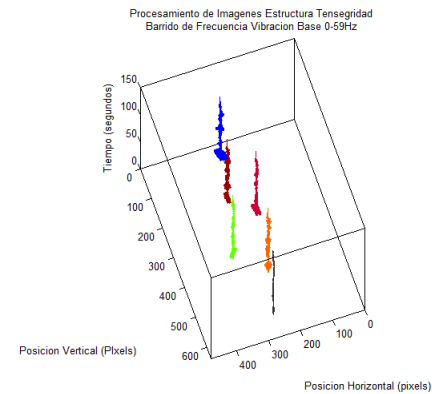


**Figure 3.** Temporary paths of 6 markers on the time axis of LEDs shown in Figure 2.

### 2.3. Frequency Response and modes of vibration of the nodes

The application developed for this work allows opening the video file and to process it frame by frame, segmenting markers and obtaining centroids for the "spots" that represent the position of each marker in each video frame (see Figure 2b). Segmentation is achieved after a smoothing process, with a threshold for the intensity and/or color-features of the pixels in the image. The remaining, isolated areas represent each LED marker in a black and white image, and the centroid coordinates for each of these areas are calculated. For greater robustness of the solution, it is possible and necessary to alter the weights within the segmentation algorithm, according to the lighting conditions in which the video was obtained (intensity threshold for the illumination corresponding to the markers). As a result of executing this application, a matrix by the components "x" and "y" of each centroid is obtained (one corresponding to each node, in each picture of the high speed video). This matrix has the information of the relative position of the nodes along the experience. The analysis of the frequency response offers direct and intuitive information for the response of a dynamic system facing an oscillatory input.

A sliding window strategy was implemented for each marker ( $m_k$ ), and for each frequency level between (1.0 Hz-60.0 Hz), to analyze response (displacements in the x-y plane) with regard to those of the base node ( $m_b$ ). The width of this window was defined in 1 second (120 samples), the output ( $m_k$ )/input ( $m_b$ ) relation was analyzed for each window displacement on the signal.

For each sliding window displacement ( $n$ ), an oscillation frequency of the structure base was estimated ( $f_{oscillator}(n)$ ) by searching the maximum level shown by the Fast Fourier Transform (FFT) of the base marker vertical displacement coordinate ( $y_{m_b}$ ) in that window ( $y_{m_b}(n:n+120)$ ). This expression is detailed in (1):

$$f_{oscillator}(n) \approx \max(|FFT(y_{m_b}(n:n+120))|) \quad (1)$$

Given the waveform of the input sign, this estimation of the oscillation frequency is indicative of the oscillation frequency assigned to the structure. In case that the dynamics of the structure affects significantly the action of the base level, and consequently the form of its FFT, the estimation of the mentioned frequency will allow to detect it as a frequency of particular interest for further analysis. The estimated frequencies are, in turn, rounded off to entire values for further utilization. Once the oscillation frequency of the structure is identified, the response frequency for each marker of interest is

obtained, in any of the two axes. To obtain a relative response to the structure base level it is necessary to subtract the respective displacement of the base marker to the vertical coordinate of each marker in the window. Since the extent of the vertical displacement in the base level changes with the frequency (for the attenuation of the actuator response, and the potential dynamic impact of the structure on itself), the response of each marker was normalized in the vertical axis, appealing to the standard deviation of the vertical displacement registered in the base, as shown in the equation (2):

$$y_{m_k}^N(n:n+120) = (y_{m_k}(n:n+120) - y_{m_b}(n:n+120))/std(y_{m_b}(n:n+120)) \quad (2)$$

Provided that the oscillatory action analyzed on the structures occur on the vertical axis, the only normalization applied to the horizontal coordinates consists in an adjustment for the effective extent of the input action expressed in (3):

$$x_{m_k}^N(n:n+120) = (x_{m_k}(n:n+120))/std(y_{m_b}(n:n+120)) \quad (3)$$

With the normalized coordinates of each marker inside the window in relation to the base ( $x_{m_k}^N(n:n+120)$ ,  $y_{m_k}^N(n:n+120)$ ), an absolute value for the FFT value was obtained for each of these signals. Prior to the FFT, mean values for each signal within the window were subtracted. These frequency responses ( $FR_{xk}$ ,  $FR_{yk}$ ), that provide information between 0 Hz and 60 Hz, were assigned to each frequency of the oscillator detected by the sliding window in that point:

$$FR_{yk}(f, f_{oscillator}(n)) = |FFT(y_{m_k}^N(i_v:j_v))| \quad (4)$$

$$FR_{xk}(f, f_{oscillator}(n)) = |FFT(x_{m_k}^N(i_v:j_v))| \quad (5)$$

Since window displacements generated multiple instances of  $FR_{xk}$  and  $FR_{yk}$ , the signals with the same associated frequency were averaged for each marker, improving overall estimations and mitigating errors in the estimation of the frequency of oscillation. With this information, it is possible to obtain two surfaces, representing the complete frequency response of each marker in the structure, facing all the assigned input frequencies. By the proposed strategy of analysis the points of significant oscillation, as well as the vibration modes that demonstrated minimal movements, were automatically, and by graphical means, identified for each structure of interest.

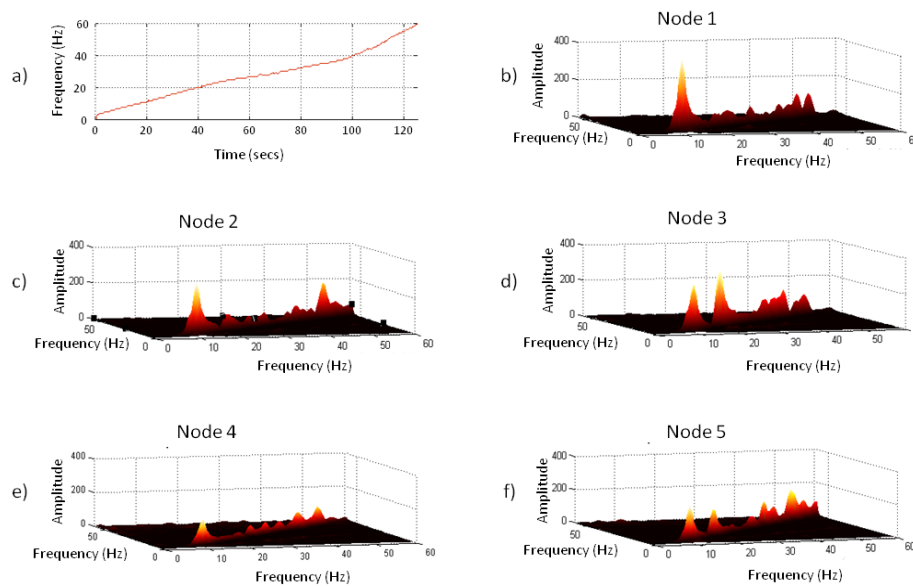


**Figure 4.** a) Frequency sweep, b)-f) Frequency-response of the structure in Figure 2, over the vertical axis, for nodes 1 through 5, respectively, compared to the base marker (node 6).

### 3. Results

#### 3.1 Frequency response of Simplex module

The results of the study of the frequency response of the Simplex module are the following. The estimation curves of the frequency of oscillation offered results compatible with the scale of input frequencies between 1.0 Hz and 60.0 Hz. Local maximum points from the surfaces, derived from the signal processing strategy, are associated to response peaks -structure resonances- whereas the minimums indicate fixed positions. As expected, the three surfaces obtained from the markers offer similar overall results, given the symmetry of the structure. The markers have a spatial distribution around the central axis of the module (actuator oscillation axis) in a radius of  $(10.0 \pm 0.1)$  cm (see figure 1a). For the three markers, a general resonance frequency is found at  $(19.2 \pm 0.1)$ , concentrated on the horizontal axis, and to a lesser degree at  $(50.2 \pm 0.1)$  Hz on the vertical axis. Table 1 summarizes relevant quantitative results derived from the experimental setup on this structure.

**Table 1.** Frequency-response for nodes 1,2 and 4 of the Simplex module

Node	Peak Frequency ( $\pm 0.1$ )Hz		Amplitude (adimensional)	
	x-axis	y-axis	x-axis	y-axis
1	19.2	-	49	-
	-	49.2	-	91
2	19.2	19.2	108	29
	-	51.0	-	76
4	19.8	19.2	45	46
	48.0	52.8	23	66

General oscillation amplitudes vary between nodes. Observable differences, like the response of node 1, for which there was no significant peak at 19.2 Hz in the vertical axis (contrary to results from analogous nodes 2 and 4), reflect differences in pre-tension states surrounding that node. The value for the second vibration mode  $(50.2 \pm 0.1)$  Hz was obtained as an average of the respective detected values among all homologous nodes (see Table 1).

Figure 5, from left to right, shows a summarized response to the input, over the horizontal axis, for nodes 1, 2 and 4 respectively. These surfaces hold similar characteristics, while their general magnitude levels and peak values are variable. Nodes 1 and 4 hold comparable response levels, while node 2 approximately doubles their amplitude. Horizontal displacements for these nodes are mostly modulated, according to the axial symmetry of rotation that defines the structure, and are therefore variably projected over the depth axis, which is not registered by the frontal camera. The standout magnitude for the response of node 2 can be explained by this fact, while other minor differences can be attributed to material flaws, as well as to involuntary assembly imperfections. Additional local maximums that were found in the horizontal axis (see Figure 5a) were not included in the table, while the selected values are a match among homologous nodes.

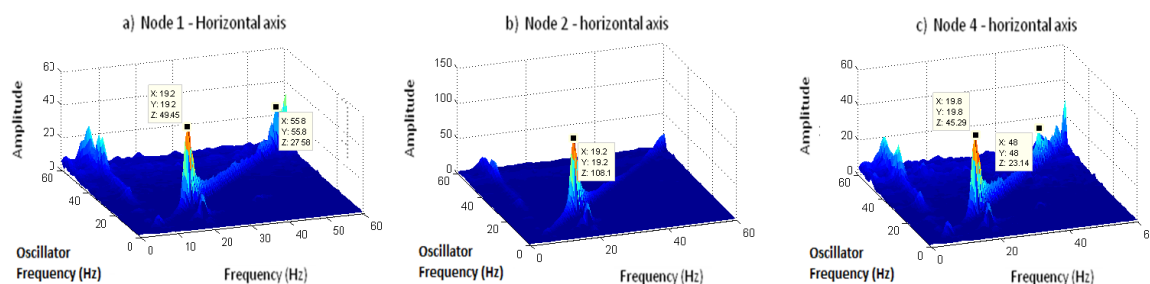


**Figure 5.** Simplex Module: a), b) and c) Frequency response in the horizontal axis, for nodes 1, 2 and 4, respectively.



### 3.2 Frequency response of the 3-bar two stages SVD tensegrity

This tower was built by piling two Simplex modules as shown in Figure 1b). The spatial orientations are opposite, being the lower anticlockwise and the superior clockwise. Once again, the frequency response of the different nodes for the Simplex module was analyzed, as described in section 2.3. Among all possible nodes, those equivalent and non-equivalent between structures can be selected to carry out comparisons. The results are shown in Table 2.

The structure presents general vibration modes, of varying magnitude, for these three nodes, at  $(16.2 \pm 0.1)$  Hz,  $(29.4 \pm 0.1)$  Hz, and  $(37.2 \pm 0.1)$  Hz. Figure 6 shows the magnitude of the frequency response from node 1, over the horizontal and vertical axis, respectively, for this two-stage structure. Node 1 shows a slightly different, more focused resonant response over its horizontal axis than the remaining nodes, with no significant peaks at 12.0 Hz, while the remaining nodes (2 and 4) display another standout point at that value. This difference is consistent with the relative placement of node 1, compared to 2 and 4, in the structure (see Figure 1). Responses show an overall increased complexity, with a larger number of feature points, all remaining within a diagonal (visible from the xy-view of the surface), representing a 1:1 ratio between oscillator frequency and peak response.

**Table 2.** Frequency response for nodes 1,2 and 4 of the 3-bar two stages SVD tensegrity

Node	Peak Frequency ( $\pm 0.1$ )Hz		Amplitude (adimensional)	
	x-axis	y-axis	x-axis	y-axis
1	16.2	16.2	389	652
	31.8	29.4	155	188
	34.8	-	202	-
	37.2	-	323	-
2	12.0	12.0	148	90
	18.0	16.2	470	236
	29.4	31.8	114	147
	37.2	37.2	441	298
4	12.0	12.0	174	79
	16.8	16.2	246	189
	29.4	29.4	102	48
	37.2	37.2	271	181

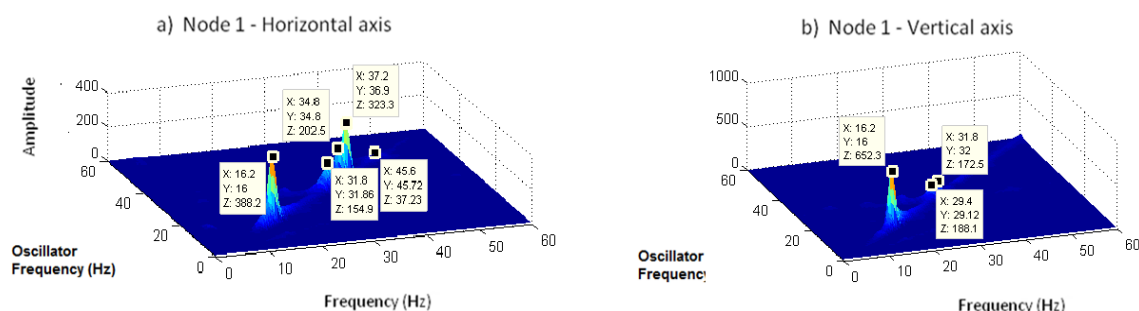


**Figure 6.** a) and b) Frequency response amplitude of node 1 in the horizontal and vertical axis, respectively, for the 3-bar two stages SVD tensegrity.

#### 3.3.1 Frequency response of the 3-bar three stages SVD tensegrity.

Frequency-response results for the 3-bar three stages SVD tensegrity tower are shown in Table 3. Since nodes 1, 4 and 6 are positioned on homologous points in the structure, which display a symmetrical behavior that was both deduced and experimentally confirmed, information from two of these nodes is not included in the Table. Significant general oscillation frequencies for this structure,

shared by these nodes, occur at  $(12.0 \pm 0.1)$  Hz and  $(21.0 \pm 0.1)$  Hz, with other, less significant peaks detected at  $(40.8 \pm 0.1)$  Hz,  $(43.8 \pm 0.1)$  Hz and  $(51.0 \pm 0.1)$  Hz.

Once again, the measured response characteristic, for both axes, is much more complex in its composition than those found in the previous sections, displaying peaks outside the 1:1 diagonal, for example at  $(10.8 \pm 0.1)$  Hz, when the input, oscillator frequency was of  $(21 \pm 0.1)$  Hz, a response at approximately one half of the frequency of the input excitation. One remaining peak of  $(1.8 \pm 0.1)$  Hz was found for  $(12 \pm 0.1)$  Hz inputs, resulting in an elaborate response of the structure to 12 Hz vibrations. Frequencies shown in Table 3 remain within the 1:1 ratio to the input signal.

Figure 7 shows four surfaces, representing the frequency response from nodes 1 and 5 of the tower. These graphs display the great variability between response characteristics, both among different nodes, as well as in the directionality of each response, for any node, which is also visible in figure 6.

**Table 3.** Frequency response for nodes 1,2 and 5 of the three-stage, 3-bar SVD structure

Node	Peak Frequency ( $\pm 0.1$ )Hz		Amplitude (adimensional)	
	x-axis	y-axis	x-axis	y-axis
1	12.0	12.0	290	256
	21.0	21.0	290	45
	-	28.2	-	86
	43.8	43.8	130	52
	51.0	51.0	55	50
2	-	12.0	-	622
	21.0	21.0	282	175
	33.0	34.2	88	67
	40.8	40.8	105	58
	51.0	51.0	60	51
5	12.6	12.0	104	492
	21.0	21.0	93	468
	35.4	33.0	73	61
	40.8	-	113	-
	-	43.8	-	94
	-	51.0	-	164

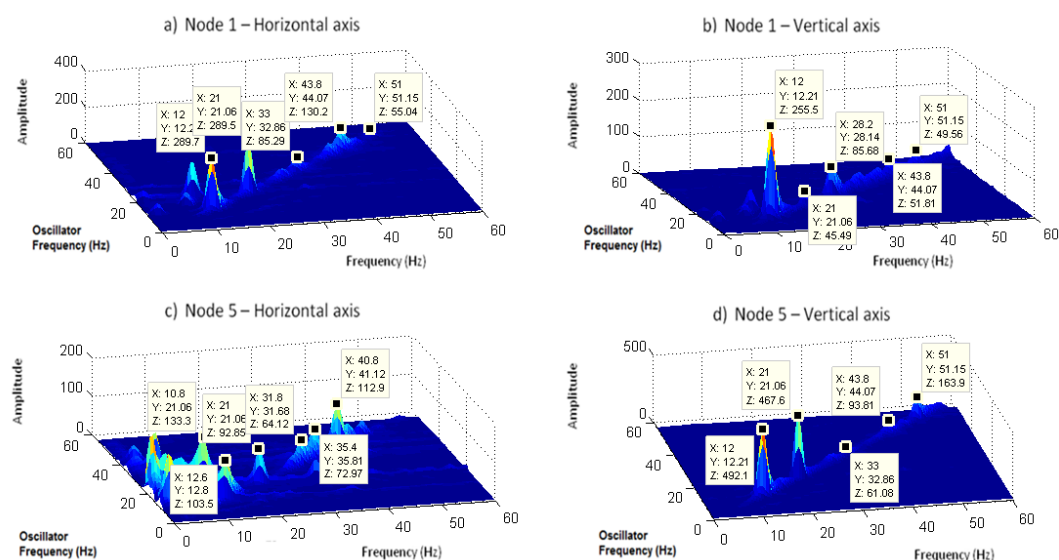


**Figure 7.** Frequency response of the 3-bar three stages SVD tensegrity (nodes 1 and 5, in both axes): Significant differences in response characteristics, between axes and nodes, are detected.



#### 4. Conclusions

In this work, a simple method for analyzing the frequency response of 3D tensegrity structure nodes (structure vibration modes) was developed, based on light emitting markers (LEDs) and a signal processing algorithm to obtain information from video images taken by a high speed camera. Each node has a characteristic and well determined resonant frequency pattern. Limitations to this method are related to its frequency range (scanning between 0 Hz and 60 Hz, with  $\pm 0.1$  Hz error), and to the fact that only oscillations parallel to the structure axis were considered. Node displacements were measured in each frame over the plane of each image.

The frequency response for a Simplex 3-bar SVD tensegrity module was measured, resulting in resonance or peak responses at  $(19.2 \pm 0.1)$  Hz and  $(50.2 \pm 0.1)$  Hz. In particular, results from this module hint at the variability of the response, which proved to be very sensitive to the material of the compressive elements. As an example, when changing aluminum to wood, for the Simplex module, the first resonant or peak frequency rises to 30 Hz. These graphs were not presented due to a lack of space.

Similar frequency responses for towers formed by two and three stages of modules were also assessed. When the modules are superposed to form towers, the number of nodes increases, but for the study, those equivalent and non-equivalent between structures were selected to carry out comparisons. These were the instrumental nodes, and some of them were compared between three structures. These results displayed an increasing complexity for the response characteristics, which in turn, and in conjunction with their sensitivity to constructive properties, highlights the value of counting with an experimental method for the assessment of real structures and prototypes, in particular, associated to more elaborate biomechanical models.

Additionally, the flexibility displayed by the response of these structures opens the possibility to “tune” them towards desirable properties for product design. These properties can, in turn, be validated through the method shown in this work.

The comparison of results to bibliography can only be accomplished with information found for the three module tower [7]. A similar tower, with a scale ratio of 2.3, was studied using 3D accelerometry, between 0 Hz and 50 Hz, and using guitar strings as tensors. As in this study, different vibration modes are found, with frequencies in the order of those found in this study. Based on a finite element model, authors associate modes to torsion and bending, and indicate the relationship in the variation of these frequencies to the pre-tension state of the structure. In the present analysis, no significant responses were found to oscillator frequencies below 12 Hz for the three-stage tower, and no evidence of “soft mode”, as indicated in [7], was found.

Future research stages can benefit from further advances in acquisition and signal-processing strategies. For example, image-processing can be used to automatically detect the oscillation frequency of the power source, taking advantage of its digital display (through optical character recognition). The addition of a second, orthogonal camera to the system can also be directly implemented as a method for 3D node tracking. Finally, alternative mechanical actuators, accepting multiple input waveforms and/or movements in different directions, can be implemented, giving place to alternative characterizations for these dynamic systems, based on the same fundamental principle of analysis presented in this work. Some examples include the precise detection dedicated to low-frequency responses and to significant changes in spatial orientation (deformations), as well as the analysis of transient responses, and fault and limit conditions, for structures and prototypes based on tensegrity models.

To summarize, we are in the presence of a structural block, with a frequency response that is highly sensitive to qualitative and quantitative variables. In turn, once these variables are determined, this response can be modeled and these parameters applied with absolute precision. This adaptive versatility, given by minimal changes to relevant variables in these tensegrity structures, is a typical feature of biological structures, at every scale.

## References

- [1] Randel L, Swanson I 2013 Biotensegrity: A unifying theory of biological architecture with applications to osteopathic practice, Education, and Research—A Review and Analysis *J Amer. Osteo. Asso.* **113** 1 34-52 <https://goo.gl/tl2IUP>
- [2] Levin S 2002 The Tensegrity-Truss as a Model for Spine Mechanics: Biotensegrity *J. Mech. Med. Biol.* **2** 03n04 375-388
- [3] Levin S 2006 Tensegrity, The New Biomechanics *Textbook of Musculoskeletal Medicine* ed Hutson M & Ellis R (Oxford: Oxford University Press) pp 69 - 80
- [4] Skelton R E and de Oliveira M 2009 *Tensegrity Systems* (Springer)
- [5] Ingber D E 2003 Tensegrity I: Cell Structure and hierarchical systems biology *J. Cell Sc.* **116** 1157-1173
- [6] Zatsiorsky 1998 *Kinetics of human motion* (Human Kinetics) p 312
- [7] Bossens F Callafon R A and Skelton R E 2004 Modal analysis of a tensegrity structure-an experimental study *Mechanical and Aerospace Engineering Dynamic Systems and Control Group* (San Diego: University of California) <http://goo.gl/CkqCHL>

## Acknowledgements

The authors wish to acknowledge the technical assistance provided by Mr. Gonzalo Fernandez. This work was carried out under - and supported in part by - Project 2062120100011BA UBACyT 2013-2016, Centro de Investigación en Diseño Industrial de Productos Complejos, *Facultad de Arquitectura, Diseño y Urbanismo, Universidad de Buenos Aires* (CIDI-FADU-UBA), y *Facultad de Ciencias Fisicomatemáticas e Ingeniería, Pontificia Universidad Católica Argentina* (UCA).